Energy & Environmental Science

PAPER

View Article Online
View Journal | View Issue

Cite this: *Energy Environ. Sci.*, 2016, **9**, 3252

A rational design of separator with substantially enhanced thermal features for lithium-ion batteries by the polydopamine–ceramic composite modification of polyolefin membranes†

Jianhui Dai,[a] Chuan Shi,[b] Chao Li,[b] Xiu Shen,[b] Longqing Peng,[b] Dezhi Wu,[c] Daoheng Sun,[c] Peng Zhang*[a] and Jinbao Zhao*[ab]

Received 26th April 2016,
Accepted 23rd August 2016

DOI: 10.1039/c6ee01219a

www.rsc.org/ees

A separator plays a crucial role in ensuring the safety in lithium-ion batteries (LIBs). However, commercial separators are mainly based on microporous polyolefin membranes, which possess serious safety risks, such as their thermal stabilities. Although many efforts have been made to solve these problems, they cannot yet fully ensure the safety of the batteries, especially in large-scale applications. Herein, we report a rational design of separator with substantially enhanced thermal features. We report how, by a simple dip-coating process, polydopamine (PDA) formed an overall-covered self-supporting film, both on the ceramic layer and on the pristine polyolefin separator, which made the ceramic layer and polyolefin separator appear as a single aspect and furthermore, this layer amended the film-forming properties of the separator. Combining the function of the ceramic and PDA, the developed composite-modified separator displays substantially enhanced thermal and mechanical stability, with no visual thermal shrink and can maintain its mechanical strength up to 230 °C when the polyethylene separator acts as the pristine separator.

Broader context

For the large-scale applications of lithium-ion batteries (LIBs), such as in electric vehicle and energy storage systems, higher safety standards are a prerequisite. In LIBs, the separator is a module that prevents direct contact of the cathode and anode electrodes, while permitting ion transport inside the cell, which is the basis of ensuring the safety of the batteries. Currently, the separators used in LIBs are mainly based on microporous polyolefin membranes, which exhibit high thermal shrinkage at elevated temperatures. Taking the conventional polyethylene (PE) separator as an example, it has a melting point of about 135 °C and readily loses its dimensional stability when exposed to high temperature above 100 °C, which could cause an internal short circuit, and consequently lead to combustion or even an explosion. Herein, we report a rationally designed separator with a composite modification. By utilizing a dip-coating strategy, polydopamine (PDA) forms an overall-covered self-supporting film both in the PE network and ceramic layer, which mechanically supports the backbone of the separator and provides resistance against thermal shrinkage. Since the self-supporting PDA film can maintain its physical strength up to 200 °C, the developed composite modified separators show excellent thermal and mechanical stability.

Introduction

Lithium-ion batteries (LIBs) are widely used in portable electronic devices due to their high energy density and excellent cycle life. Furthermore, LIBs are also regarded as the most competitive power source for large-scale battery applications, such as in electric vehicle (EV) and energy storage systems (ESSs),[1–3] provided that their safety and cost can be substantially improved.[4–6] In LIBs, a separator plays the crucial role of preventing contact of the cathode and anode electrodes, while at the same time permitting ion transport inside the cell.[7] Currently, the separators used in LIBs are mainly based on microporous polyolefin membranes, such as polypropylene (PP) and polyethylene (PE), because of their good mechanical strength and chemical stability. However, these polyolefin membranes exhibit high thermal shrinkage at elevated temperatures, which could cause an internal short circuit in the case of an unusual heat generation, and could consequently lead to an outbreak of fire or even an explosion. Moreover, the large

[a] *School of Energy Research, College of Energy, Xiamen University, Xiamen, 361005, P. R. China. E-mail: jbzhao@xmu.edu.cn, pengzhang@xmu.edu.cn*
[b] *State Key Lab of Physical Chemistry of Solid Surfaces, Department of Chemistry, Collaborative Innovation Centre of Chemistry for Energy Materials, College of Chemistry and Chemical Engineering, Xiamen University, Xiamen, 361005, P. R. China*
[c] *School of Aerospace Engineering, Xiamen University, Xiamen, 361005, P. R. China*
† Electronic supplementary information (ESI) available. See DOI: 10.1039/c6ee01219a

disparity in polarity between the polyolefin separators and the organic electrolyte solvents leads to poor wettability, which hinders the absorption of electrolyte solutions into the microporous membrane. As a result, these polyolefin separators always suffer from lower conductivity, and a fade in both capacity and power capability upon cycling.[8,9]

To overcome these problems, many efforts have been carried out. One alternative option is to utilize solid electrolytes.[10–12] However, the resulting relatively low room temperature ionic conductivity and inferior mechanical strength are not satisfactory to meet the practical needs.[13] Midway between solid electrolytes and liquid electrolytes are the so-called gel polymer electrolytes (GPEs), which simultaneously possess both the cohesive properties of solids and the diffusive transport properties of liquids,[14] and have a superior electrolyte retention ability, which is vital for the safety of the batteries.[15,16] There are many pioneering works on forming composite GPEs utilizing materials such as glass fibre, nonwoven mats, cellulose and single ion polymer electrolytes.[17–20] However, the poor mechanical strength still limits their further applications.[14] The most practical choice could be modification of the commercial polyolefin separators, amongst which the surface coating of the polyolefin separator with inorganic ceramics, such as Al_2O_3 and SiO_2, has been proven to be an efficient approach.[7,8] However, restricted by the binder component and construction of the ceramic layer, improvement of the thermal properties of the separator *via* ceramic coating is limited. Here, on the one hand, the binders used to form the ceramic coating layer, such as, polyvinylidene fluoride (PVDF), polyvinylidene fluoride-hexafluoropropylene (PVDF-HFP), polymethyl methacrylate (PMMA),[21–24] show a high shrinkage at high temperature and readily swell and form a gel in liquid electrolytes, resulting in exfoliation of the coating layer from the separator, and thus the ceramic layer shows poor film-forming properties.[25] On the other hand, polyolefin separators also lose their mechanical strength at elevated temperature, which could cause a rupture of the separators, resulting in a short circuit, even in a high heat resistance binder system such as styrene-butadiene rubber (SBR) and carboxymethyl cellulose (CMC), as shown in our previous works.[26–28]

Living things in nature have developed extraordinary material properties that may be useful in many technological applications. In recent years, many significant efforts have been put into developing applications of biomass-derived materials in electrochemical energy storage techniques.[29] Inspired by the composition of adhesive proteins in mussels, the Messersmith group found that dopamine, a commercially available chemical, containing both catechol and amine groups, can carry out self-polymerization and produce adherent polydopamine (PDA) coatings on a wide variety of materials.[30] Based on this finding, in recent research, Ryou *et al.* reported a surface modification method for PE separators using PDA. The PDA-coated separators showed good electrochemical properties and performed well in LIBs.[31,32] Considering its strong adhesive capacity, PDA was also used as an intermediate layer for further functionalization of the separators.[33–36] However, there have been little research carried out to study the influence of the PDA on the thermal features of the separator. Since the structural subunits of PDA resemble those of eumelanin, which can maintain its physical strength up to 200 °C,[37,38] an overall coating of PDA suggests a clue to enhancing the thermal and mechanical stability of polyolefin separators.

In the present study, we developed a rationally designed separator with a composite modification by introducing an organic–inorganic hybrid coating layer to improve the thermal and mechanical stability. By utilizing a simple dip-coating process, as schematically demonstrated in Fig. 1, we showed that PDA could form an overall-covered self-supporting film, both on the ceramic layer and on the pristine polyolefin separator, which makes the ceramic layer and polyolefin separator appear as a single aspect, and furthermore, this could amend the film-forming properties of the separator. Combining the function of the ceramic and PDA components, the developed composite-modified separator displayed substantially enhanced thermal and mechanical stability. In this paper, we choose SiO_2 as the ceramic and PE separator (20 μm, manufactured by a wet process, Asahi Kasei Corp.) as the pristine separator. Characterization and measurement of the various separators were carried out. The cycling performance and C-rate capability of the cells with the composite-modified separator were also investigated and compared to those of a cell assembled with a pristine PE separator and only a ceramic-coated separator. It is necessary to point out that the developed modification strategy is universally efficient for all kind of ceramics and polyolefin separators, which should be very promising for its industrialization.

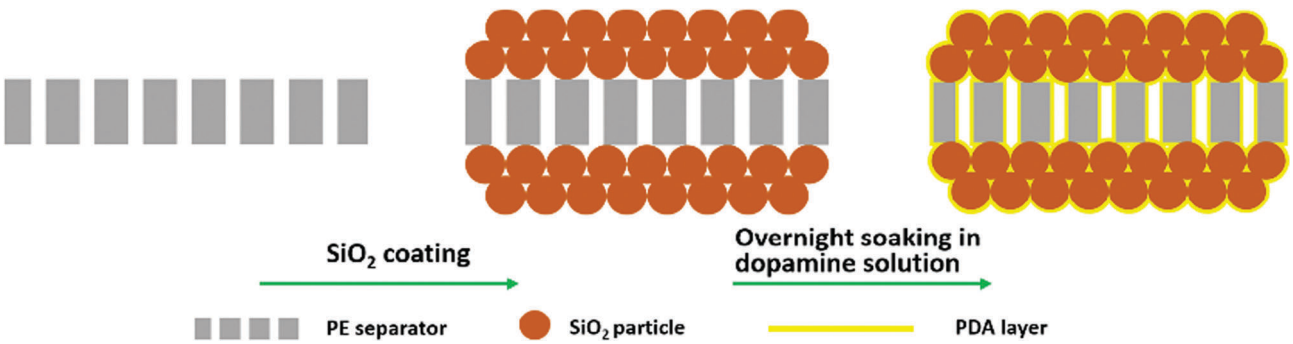

Fig. 1 Schematic illustration of the preparation of the composite-modified separator with a simple dip-coating process.

Experimental section

Preparation of the composite-modified separator

The SiO_2 particles were prepared using the Stöber method.[39] The coating slurry was prepared by the method in our previous works,[26–28] and was applied to both sides of the PE separator using an automatic film-coating machine (Shanghai Environmental Engineering Technology Co., Ltd). The SiO_2-coated PE separator (PE-SiO_2) was dried at room temperature for 1 h, and then additionally dried under vacuum conditions at 60 °C for 12 h. The prepared PE-SiO_2 separators were immersed into the dopamine solution (10 mM) with ethanol and Tris buffer solution (pH = 8.5) as the co-solvents (CH_3CH_2OH : buffer = 1 : 1 by volume).[30,31] After an overnight soaking, the separators were taken out, rinsed with water and dried under vacuum conditions, obtaining the PDA-treated SiO_2-coated PE separators (PE-SiO_2@PDA).

Electrode preparation and cell assembly

The positive electrode was prepared by coating the *N*-methylpyrrolidine (NMP)-based slurry containing 90 wt% Li_2MnO_4 (Qingdao Shuangxing Co., Ltd), 5 wt% super-P carbon and 5 wt% PVDF on aluminium foil and drying in a vacuum oven at 80 °C for 12 h. A lithium half-cell (2016 coin) was assembled by sandwiching a separator between a Li_2MnO_4 cathode and a lithium-metal anode. The electrolyte was composed of 1 M $LiPF_6$ in ethylene carbonate (EC)/diethyl carbonate (DEC)/dimethyl carbonate (DMC) (1 : 1 : 1 volume, Zhangjiagang Guotaihuarong New Chemical Materials Co., Ltd). The cell assembly was carried out in a glove box (M. Braun GmbH) filled with argon gas.

Characterization and measurements

The morphologies of the SiO_2 particles and separators were investigated using field emission scanning electron microscopy (FE-SEM, Hitachi S4800, Japan). The chemical composition of the separators was determined by Fourier transform infrared spectroscopy (FT-IR) using a Nicolet IS5 spectrometer (Thermo Fisher Scientific Inc.) in the range of 400–4000 cm^{-1} and by energy dispersive X-ray spectroscopy (EDX, Hitachi S4800, Japan). To investigate the thermal stability, the thermal shrinkage of the separators was determined by measuring the dimensional change (area-based, 2 cm square) after heat treatment at various temperatures for 0.5 h, and the shrinkage was calculated according to the following equation:

$$\text{Thermal shrinkage (\%)} = (S_0 - S)/S_0 \times 100\% \quad (1)$$

where S_0 and S are the areas of the separator before and after the heat treatment, respectively. To examine the mechanical properties, the mechanical strength was evaluated using the Universal Material Testing Machine (UTM-4000, SUNS, Shenzhen) at a strain rate of 1.66 mm s^{-1}, before and after the separators were treated at various temperature for 0.5 h, respectively. DSC measurements were carried out on a Model STA 449 instrument (NETZSCH Machinery and Instruments Co., Ltd) at a heating rate of 10 °C min^{-1} from 35 °C to 500 °C. The electrolyte uptake (EU) was calculated as follows:

$$\text{EU (\%)} = (W - W_0)/W_0 \times 100\% \quad (2)$$

where W_0 and W are the weights of the separators before and after the immersion in the liquid electrolyte, respectively. The porosity was determined by the weight of hexadecane absorbed in the pores of the separator, and the porosity was calculated by assuming that the volume occupied by hexadecane is equal to the porous volume of the separator, *i.e.*:

$$\text{Porosity (\%)} = (\Delta m/\rho)/V_0 \quad (3)$$

where Δm is the mass difference of the separator between after and before the absorption with hexadecane, ρ is the density of the hexadecane and V_0 is the volume of the separator, which includes the polymer volume and porous volume. The surface hydrophilic properties of the separators were measured using a contact angle goniometer (Powereach JC2000C1, Shanghai Zhongchen Digital Technique Equipment Co., Ltd). The ionic conductivity was measured by sandwiching a separator between two stainless steel blocking electrodes, and AC impedance measurements were then carried out using an electrochemical working station (AutoLab, Sino-Metrohm Technology Ltd) in the frequency range of 1 Hz–100 kHz, to obtain the bulk resistances (R_b) of the blocking type cells. The ionic conductivity was calculated using the equation:

$$\sigma = L/(R_b \times A) \quad (4)$$

where σ is the ionic conductivity, R_b is the bulk resistance, L is the thickness of the separator and A is the area of the stainless steel electrode (because the area of the separator is larger than that of the steel electrode).

To compare the safety performance of the cells assembled with the PE separator, PE-SiO_2 separator and PE-SiO_2@PDA separator, open circuit voltage (OCV) measurements were carried out. Pouch cells were assembled by sandwiching the separators between Li_2MnO_4 cathodes and graphite anodes. The cells were charged to 4.2 V at room temperature and then placed into a dying oven at 170 °C, then the OCV of the cells as a function of time was simultaneously monitored using an electrochemical working station (AutoLab, Sino-Metrohm Technology Ltd). To study the cycle performance, the cells were cycled with a battery testing system (LAND-V34, Wuhan LAND Electronics Co., Ltd) under the following regime. The cells were charged at a current density of 0.5C up to a cut-off voltage of 4.3 V, followed by a constant-voltage charge with decreasing current until the charge current equalled 10% of the initial current (namely, the CCCV mode). Second, the cells were discharged to a cut-off voltage of 3.0 V at the same current density (namely CC mode). In order to investigate the C-rate capability, the cells were cycled at several discharging current densities ranging from 0.5 to 10C (0.5C, 1.0C, 2.0C, 5.0C and 10C) while maintaining the charge current density at a rate of 0.5C (CCCV mode for the charge and CC mode for the discharge between 3.0 and 4.3 V).

Results and discussion

Fig. 2(a) and (b) shows the FE-SEM image of SiO_2 particles obtained by the Stöber method. The SiO_2 particles had uniform spherical shapes with a diameter of about 200 nm. The SiO_2 particles synthesized were coated onto both sides of a PE separator. Fig. 2(c) presents the photographic image of the pristine PE separator (left), the PE-SiO_2 separator (middle) and the PE-SiO_2@PDA separator (right). The formation of PDA undergoes a very complicated auto-redox process as well as the generation of a series of complex intra- and intermolecular reactions during the self-polymerization process.[30,36,40,41] After overnight dipping, the colour of the separators changed from white to dark brown, which implies the successful generation of PDA.[30–32] The surface morphologies of the PE-SiO_2 separator and PE-SiO_2@PDA separator are presented in Fig. 2(d) and (e) and Fig. 2(g) and (h). The SiO_2 particles were uniformly distributed on the surface of the PE separator without any agglomeration. After PDA treatment, the surface of the separator kept its homogeneous morphology. The SiO_2 particles became coarse, with some PDA particles stuck to them. The cross-sectional morphologies shown in Fig. 2(f) and (i) reveal that the SiO_2 particles were deposited uniformly on both sides of the PE separator, and that the coating layer was approximately 3 μm thick on each side. The PDA layer scarcely changed the thickness of the ceramic layers. Quantitative measurements showed that the weight change of the separator before and after the PDA coating was just about 0.12 mg cm^{-2}.

To confirm the generation of PDA, the characterizations of FT-IR and EDX were carried out. As shown in Fig. 3(a), for the PDA synthesized by the same process without adding a separator, peaks at 1610 cm^{-1} and 1510 cm^{-1} could be observed, which are attributed to the overlap of the C=C resonance vibration in the aromatic ring and the N–H bending vibration, respectively.[42–44] For the PE-SiO_2 separator, all the peaks originating from the bare PE separator and SiO_2 were still preserved, and another peak at 1630 cm^{-1} corresponded to the bending motion of H–O–H. After immersion in the dopamine solution, compared to the PE-SiO_2 separator, the PE-SiO2@PDA separator exhibited new peaks: a peak at 1510 cm^{-1}, originating from PDA, and the overlapping peaks at 1610 cm^{-1} and 1630 cm^{-1} shifted to 1625 cm^{-1}. Thus, the FT-IR spectrum provides evidence for the generation of PDA. The EDX spectra in Fig. 3(b) further confirmed the change of the surface composition resulting from the PDA coating. While the PE-SiO_2 separator only had C and Si peaks, the PE-SiO_2@PDA separator exhibited newly appearing N peaks, thereby indicating the formation of PDA.[31] In addition, to ensure that the PDA coating took place over all the ceramic layer and deep inside the PE separator, EDX element mapping analysis was conducted for the separators cross-section. As shown in Fig. 4, the distribution of Si and C strictly corresponded with the area of the ceramic layer and the PE layer, while elemental

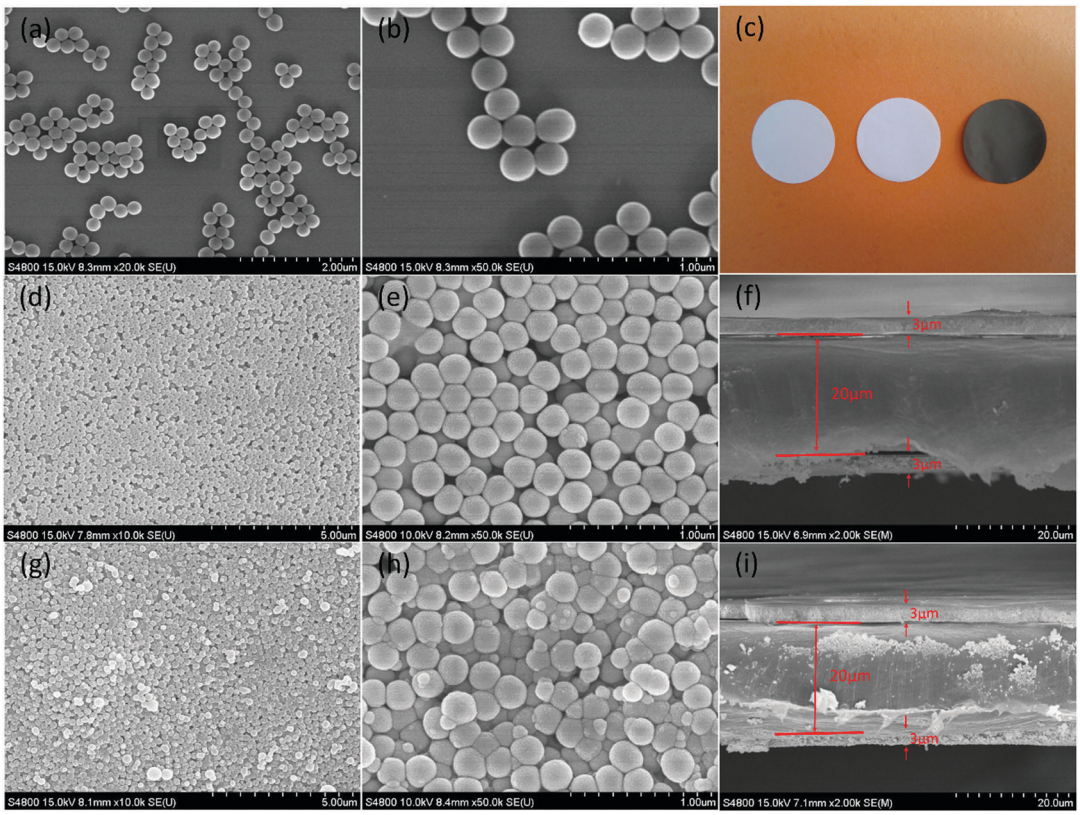

Fig. 2 (a and b) SEM images of the SiO_2 particles, (c) photographic image of the pristine PE separator (left), PE-SiO_2 separator (middle) and PE-SiO_2@PDA separator (right); SEM images of the surface and cross-section of (d)–(f) the PE-SiO_2 separator and (g)–(i) the PE-SiO_2@PDA separator.

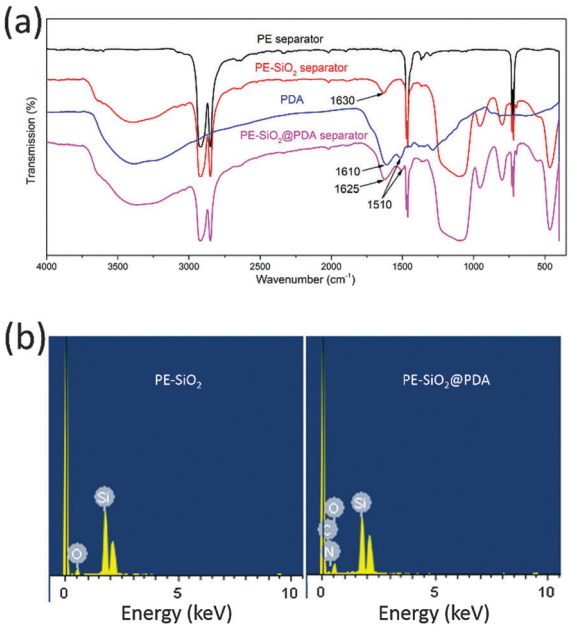

Fig. 3 (a) The FT-IR spectra and (b) EDX spectra.

N was distributed homogeneously throughout the cross-section, thus verifying that the PDA coating was complete throughout the entire separator. As illustrated in Fig. 1, the overall coating of PDA makes the ceramic layer and PE separator appear as a single aspect. Furthermore, PDA formed an overall-covered self-supporting film.

The most essential function of a separator is preventing direct contact of the cathode and anode electrodes, while at the same time permitting ion transport inside the cell. Thus, the separators should be chemically, thermally and mechanically stable. Otherwise, the anode and cathode would contact each other, causing an internal short circuit, potentially leading to a thermal runaway, even combustion or an explosion, especially in the case of abuse of the system. However, the PE separator has a melting point of about 135 °C and readily loses dimensional stability when exposed to a high temperature above 100 °C.[7,9] Surface coating with ceramic could improve the dimensional stability of the separator, albeit not quite enough for ensuring the safety of LIBs, especially for large-scale applications, since the components and construction of the ceramic layer restrict its film-forming properties at high temperature. In order to investigate the influence of the PDA treatment on the thermal-resistant characteristics, the thermal shrinkage behaviour was surveyed by measuring the dimensional change (area-based) after subjecting the separators to heat treatment at a series of temperatures from 100 °C to 230 °C for 0.5 h respectively. The results are shown in Fig. 5(a). The bare PE separator began to shrink above 100 °C, and had a shrinkage of 5.0% at 110 °C while the PE-SiO_2 separator and PE-SiO_2@PDA separator remained intact. The PE-SiO_2 separator retained its integrity until 140 °C, but then shrank 5.0% at 150 °C. The PE-SiO_2@PDA separator, on the other hand, had no visual shrinkage even at 230 °C. Fig. 5(b)–(d) show the photographs of the pristine PE separator, the PE-SiO_2 separator and the PE-SiO_2@PDA separator (2 cm square) before and after being subjected to heat treatment at 170 °C for 0.5 h. It can be seen that at 170 °C, the PE-SiO_2@PDA separator had no visible shrinkage, while the pristine PE separator and PE-SiO_2 separator had a shrinkage of 82.3% and 28.4%, respectively. Fig. 5(e) shows that even at 220 °C, the dimensions of the PE-SiO_2@PDA separator still remain intact. At 230 °C, a serious rupture phenomenon occurred, although there was no visual shrinkage for the PE-SiO_2@PDA separator. To further understand the function of the ceramic and PDA, we further investigated the thermal stability of the PE@PDA separator, which was prepared by the same process but without a ceramic layer. The results are shown in Fig. S1 (ESI†). It can be observed that PDA modification does improve the thermal stability of the PE separator. However, without a ceramic layer, the PE@PDA separator began to shrink at temperatures up to 120 °C. As shown in Fig. S1(b) (ESI†), the PE@PDA separator displayed a thermal shrinkage of 78.2% at 170 °C. The experimental results indicate that the substantially improved thermal stability is not definitely derived from the simple collection of the respective features of the ceramic and PDA, but rather results from a synergistic effect from the combination of the functions of the ceramic and PDA.

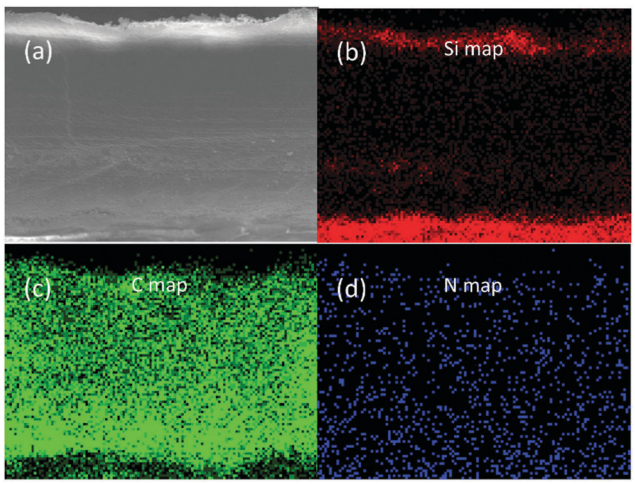

Fig. 4 (a) SEM image of the corresponding PE-SiO_2@PDA separator cross-section and elemental mapping of (b) Si (c) C (d) N.

The mechanical stability of separators is very important for ensuring the safety of the batteries, especially at elevated temperatures. However, the mechanical strength of the separator will also reduce at elevated temperatures, which may cause a rupture and loss of integrity, leading to an internal short circuit. To investigate the influence of the composite modification on the mechanical properties, mechanical strength measurements were conducted before and after the separators were subjected to heat treatment at a series of temperatures from 130 °C to 230 °C for 30 min respectively. Fig. 6(b) shows the stress–strain curves of the PE-SiO_2 separator and PE-SiO_2@PDA separator before being subjected to the heat treatment. It can be observed that after PDA treatment, both the tensile strength and

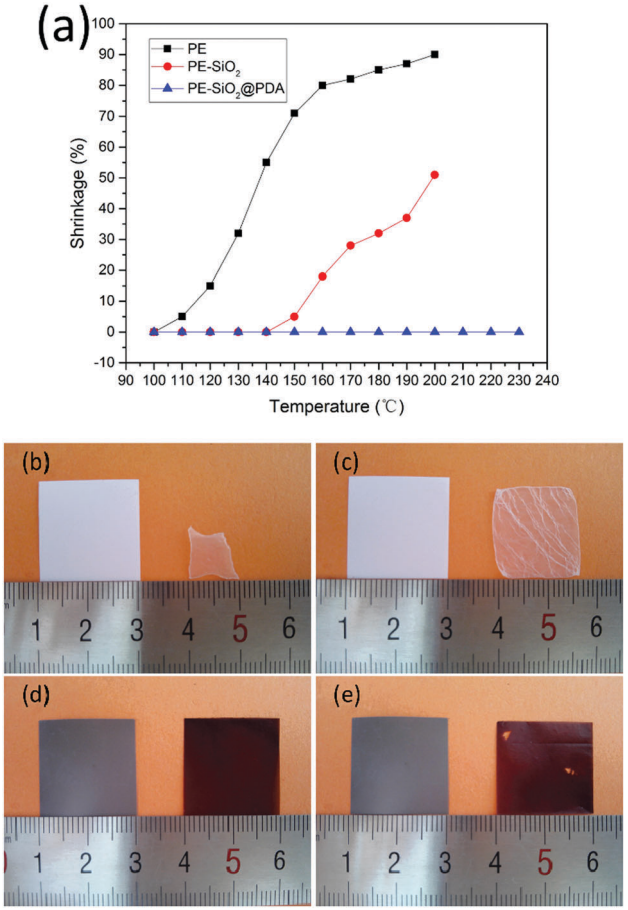

Fig. 5 (a) Thermal shrinkage of the pristine PE separator, PE-SiO_2 separator and PE-SiO_2@PDA separator as a function of temperature, Dimensions of the separators before and after being subjected to heat treatment at 170 °C for 30 min (b) the pristine PE separator, (c) the PE-SiO_2 separator, (d) the PE-SiO_2@PDA separator and (e) the PE-SiO_2@PDA separator at 220 °C.

elongation were strengthened, which would be very significant for battery manufacturing processes.[45] As shown in Fig. 6(a), the tensile strength of the separators decreased as the temperatures were raised. For the PE-SiO_2 separator, it lost its mechanical strength completely at 180 °C. However, the PE-SiO_2@PDA separator kept its mechanical strength until 230 °C. To understand the mechanism for the separators losing their mechanical strength, SEM images of the surfaces of the PE-SiO_2 separator and PE-SiO_2@PDA separator after the heat treatment at the temperatures before and after losing the mechanical strength were measured. As shown in Fig. 6(c) and (d), at 170 °C, the surface of the PE-SiO_2 separator retained its pristine morphology, illustrating that the ceramic layer and the PE layer kept their statuses, respectively, thus the separator can form a self-supporting film. However, at 180 °C, it can be observed that the melted-down PE layer has permeated into the interspaces of the ceramic layer, such that the separator cannot self-support to form a stubborn film, and hence it loses its mechanical strength. For the PE-SiO_2@PDA separator, the same phenomenon can be observed at temperatures of 220 °C and 230 °C, respectively (Fig. 6(e) and (f)). To further understand the function of the PDA treatment for promoting the thermal and mechanical stabilities of the separator, DSC measurements were carried out for the PDA synthesized by the same process without adding a separator. The DSC curve in Fig. 6(a) shows that the outset of the endothermic peak was at 206.6 °C, which was supposed to be the temperature for PDA to begin to melt down and lose its physical strength and for the self-supporting PDA film to lose its film-forming properties. Further investigating the change of the tensile strength of the PE-SiO_2@PDA separator as a function of temperature, it was found that there are two sharp declines in the mechanical strength. Obviously, the first one starts at 130 °C, caused by the melting of the PE layer, which was also observed for the PE-SiO_2 separator. The second one started at 210 °C, and should correspond to the change of the PDA, which is consistent with the result from the DSC measurements. Since there are strong intermolecular interactions, such as hydrogen-bonding and π–π interactions,[32,46,47] the PDA layer can form a stubborn self-supporting film, which can mechanically form the overall backbone of the separator and maintain the mechanical strength up to the temperature at which PDA loses its physical stability.

The PDA layer substantially promotes the thermal and mechanical stability of the separator, which is very important for ensuring the safety of LIBs. The enhanced thermal and mechanical stability are due to the overall-covered self-supporting PDA film in the PE network and ceramic layer, which mechanically form the backbone of the PE separators and provides resistance against thermal shrinkage. As demonstrated in Fig. 1, PDA forms an overall-covered self-supporting film both on the ceramic layer and pristine polyolefin separator, which makes the ceramic layer and PE separator appear as a whole aspect, and furthermore, this can amend the film-forming properties of the separator. By combining the functions of the ceramic and PDA components, the developed composite-modified separator displays substantially enhanced thermal and mechanical stability.

Due to their hydrophobic surface character and low surface energies, PE separators have an intrinsically poor compatibility with conventional liquid electrolytes, which not only impairs the power performance and cycle lives of LIBs, but also creates problems in battery manufacturing processes.[7,45] Both the surface ceramic coating and PDA treatment of the PE separator were proved to be an effective approach to change the surface properties and enhance the wettability of the separators. In order to investigate the effect of the PDA–SiO_2 composite layer on the wettability of the separators, contact angle measurements with water droplets were conducted. As shown in Fig. 7, the static water contact angles of the separators decreased after each step of the modification process: 88 ± 1.2° for the PE separator, 43 ± 2.7° for the PE-SiO_2 separators and 36 ± 1.7° for the PE-SiO_2@PDA separators. The decreased contact angle implies that after PDA treatment, the PE-SiO_2@PDA separator had a better wettability compared to the PE-SiO_2 separator. For greater quantitative testing, the electrolyte uptake amounts were measured. The results are summarized in Table 1. The PE separator had an uptake of 54 ± 2.7%. As expected, the uptake amount of the PE-SiO_2 separator increased

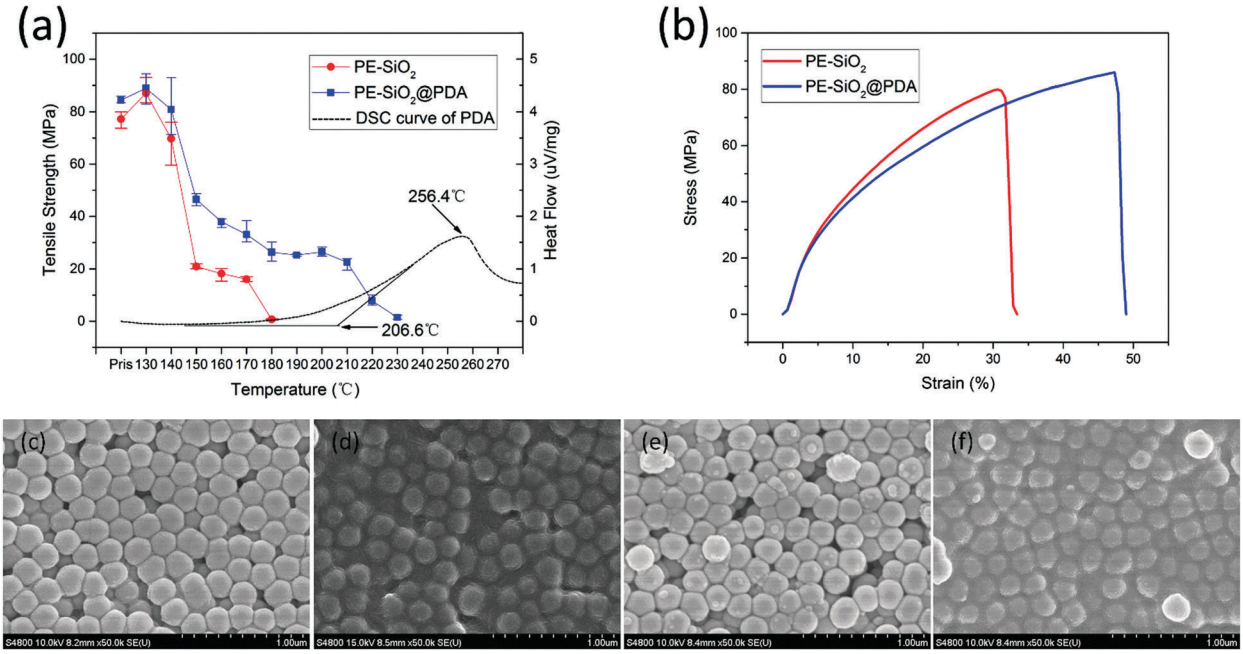

Fig. 6 (a) Tensile strength of the PE-SiO_2 separator and PE-SiO_2@PDA separator as a function of temperature, and DSC curve of PDA, (b) stress–strain curves of the PE-SiO_2 separator and PE-SiO_2@PDA separator before being subjected to heat treatment, SEM images of the surface of (c) and (d) the PE-SiO_2 separator after heat treatment of 170 °C and 180 °C and (e) and (f) the PE-SiO_2@PDA separator after heat treatment of 220 °C and 230 °C.

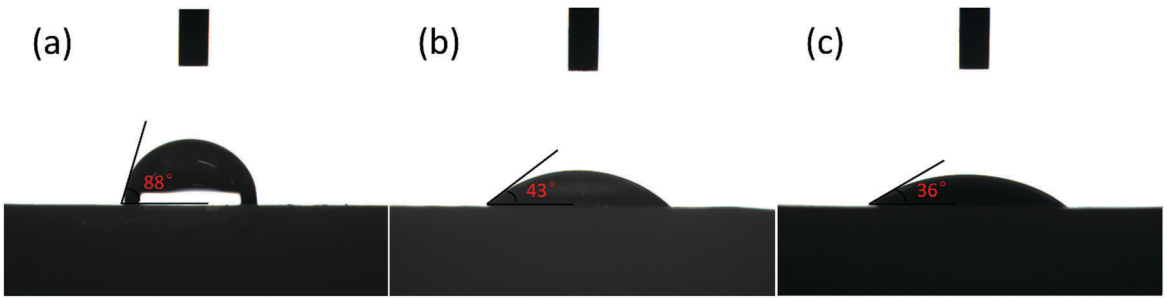

Fig. 7 Contact angle images of (a) the PE separator (b) the PE-SiO_2 separator and (c) the PE-SiO_2@PDA separator.

Table 1 Physical properties of the PE separator, PE-SiO_2 separator and PE-SiO_2@PDA separator

Separator	PE	PE-SiO_2	PE-SiO_2@PDA
Thickness (μm)	20	26	26
Contact angle (°)	88	43	36
Electrolyte uptake (%)	54	89	80
Porosity (%)	43.8	47.5	44.1
Ionic conductivity (S cm^{-1})	8.17×10^{-4}	1.20×10^{-3}	9.81×10^{-4}

to 89 ± 3.2%, while the PE-SiO_2@PDA separator had a little lower uptake of 80 ± 4.3%. As is well known, the ionic conductivities mainly rely on the uptake amounts of liquid electrolyte in the separators. As expected, the ionic conductivity increased from 8.17×10^{-4} S cm^{-1} for the PE separator to 1.20×10^{-3} S cm^{-1} for the PE-SiO_2 separator, while the PE-SiO_2@PDA separator had a little lower value at 9.81×10^{-4} S cm^{-1}. Compared to the PE-SiO_2 separator, the PE-SiO_2@PDA separator had a better wettability, while it had a lower uptake amount and ionic conductivity. To further understand the reason for this phenomenon, the porosity was measured. As shown in Table 1, the PE separator has a porosity of 43.8 ± 0.5%. The porosity of the PE-SiO_2 separator had a higher value of 47.5 ± 0.3%. After the PDA modification, the PE-SiO_2@PDA separator displayed a lower porosity of 44.1 ± 0.8% than the PE-SiO_2 separator. Obviously, the reason for this could be that the PDA takes up parts of the interspaces of the separators and reduces the porosity. However, the PE-SiO_2@PDA is still superior to the PE separator. Also, for practical application, a PE separator with a high porosity will eliminate the effects of the take-up problem.

The OCV behaviour of a cell is a direct reflection of the safety performance of the cell. If there is a thermal shrinkage or rupture of the separator, the anode and cathode could come into contact directly, resulting in a sudden OCV drop. To further investigate the safety performance of the cells assembled with the PE separator, the PE-SiO_2 separator and the PE-SiO_2@PDA

separator, OCV experiments were performed. The pouch cells (as shown in Fig. S2, ESI†) were fully charged to 4.2 V, and the OCV was continuously monitored at 170 °C. As shown in Fig. 8(a), the OCV of the cell assembled with the PE separator dropped sharply to 0 V only after 75 s. Similarly, the cell with the PE-SiO_2 separator showed an OCV sharp drop at 487 s. In contrast, the cell with the PE-SiO_2@PDA separator did not exhibit an OCV sharp drop throughout the entire measurement period. It is worth noting that the slow voltage drop during the measurement was due to the self-discharge of the cells caused by the dissolving of the manganese at high temperature. Fig. 8(b) shows the photographic image of the separators after the OCV measurement. It can be observed that the PE separator and PE-SiO_2 separator displayed a large shrinkage, while the shrinkage for the PE-SiO_2@PDA separator was not obvious. The excellent thermal stabilities of the PE-SiO_2@PDA separator would play an important role in ensuring the safety of LIBs, and are promising for battery applications requiring high safety features.

The effects of the modifications on the cycle performances of the cells with different separators were also studied. Fig. 8(c) shows the discharge capacities as a function of the cycle number of the cell with the PE separator, PE-SiO_2 separator and PE-SiO_2@PDA separator. After 200 cycles operated at a 0.5C rate of charge and discharge, the cells with the PE separator, PE-SiO_2 separator and PE-SiO_2@PDA separator maintained 93.8%, 93.3% and 93.9%, respectively, of their initial capacities. The cycling data indicate that the PDA–SiO_2 composite modification has no visible negative impact on the battery performance, and that the PDA–SiO_2 hybrid layer is robust enough for long-term cell operation. To further investigate the cell performance at elevated temperatures, we tested the cycling performance of the cells at 60 °C, with $LiFePO_4$/Li metal and 1 M LiBOB in propylene carbonate (PC) as the electrolyte. As shown in Fig. S3 (ESI†), the cell with the developed separator displayed a good cycling performance at 60 °C, indicating that the as-designed separator can keep its structure and work normally at an elevated temperature.

The composite modification was further electrochemically examined, focusing on the rate capability. As clearly shown in Fig. 8(d), at the lower discharge rates of 0.5C and 1C, the three kinds of separator showed a similar rate performance, which is consistent with the results from the cycle performance.

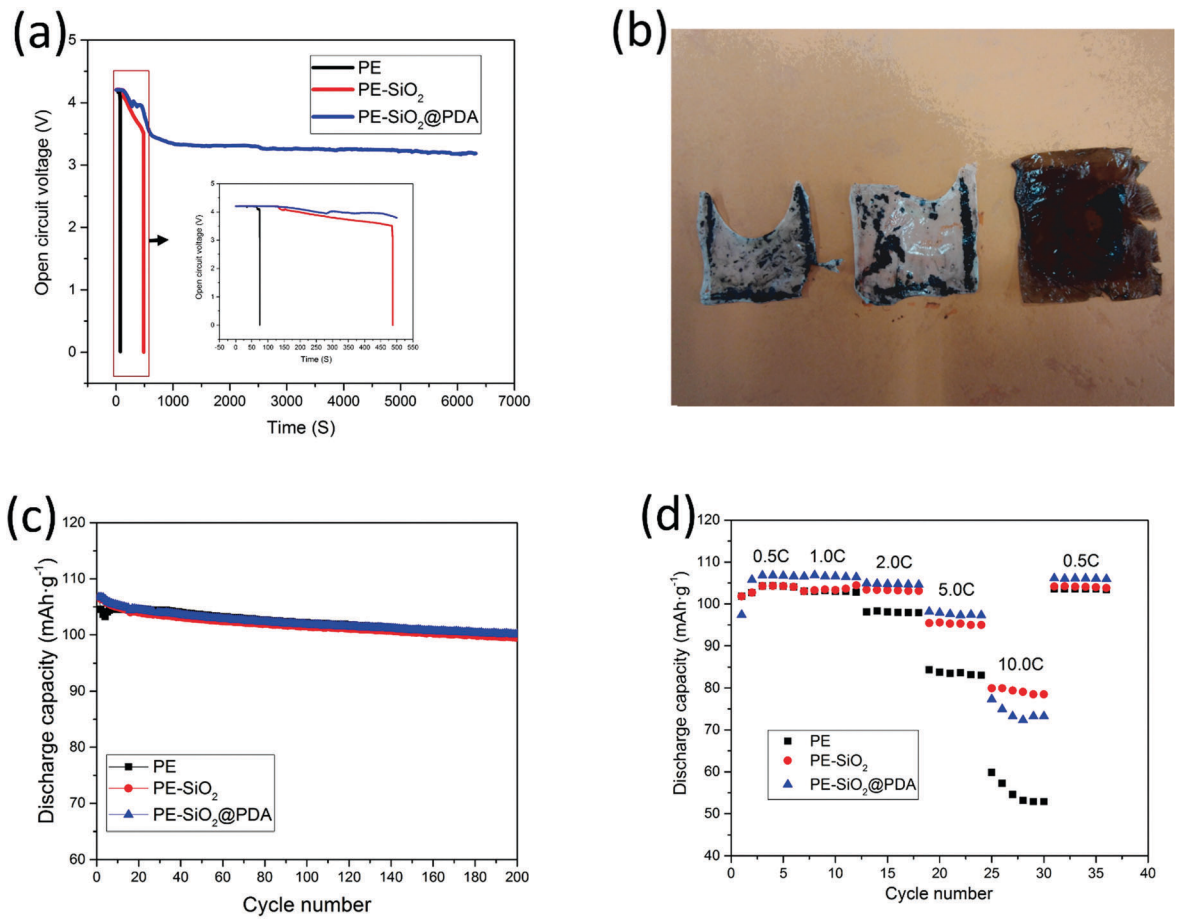

Fig. 8 (a) OCV measurement of pouch cells assembled with the PE separator, PE-SiO_2 separator and PE-SiO_2@PDA separator at 170 °C (the inset shows the enlarged profiles), (b) photographic image of the separators after the OCV measurement, (c) Cycle performance of coin cells assembled with the PE separator, PE-SiO_2 separator and PE-SiO_2@PDA separator and (d) C-rate capability of coin cells assembled with the PE separator, PE-SiO_2 separator and PE-SiO_2@PDA separator.

Upon the increase of the current rate, the discharging capacity of the cell with the pristine PE separator dropped drastically. The discharge capacity at 10C was 50.8% of the discharge capacity at 0.5C. By contrast, both the PE-SiO_2 separator and PE-SiO_2@PDA separator cells exhibited an improved capacity retention. At a rate of 10C, the PE-SiO_2 separator and PE-SiO_2@PDA separator cells maintained 75.4% and 68.7% of their initial capacity, respectively. Furthermore, with deeper observation, it could be found that at lower discharge rates, the PE-SiO_2@PDA separator performed superiorly to the PE-SiO_2 separator, while the reverse result was obtained at the rate of 10C. These results coincide with the data of the electrolyte uptake, the porosity and the ionic conductivity experiments. At a lower rate, both the ionic conductivities of the PE-SiO_2 separator and PE-SiO_2@PDA separator are high enough to support the current density. Since the surface of PE-SiO_2@PDA has a better wettability property, which facilitates transport of the lithium ions between the separator and the electrode, the PE-SiO_2@PDA displays a little higher capacity at lower rates. However, at a high rate of 10C, the resistance of the electrolyte becomes the rate determining factor, and the higher ionic conductivity of the PE-SiO_2 separator promises a better rate performance. Once again, for practical application, taking a high porosity PE separator as the base membrane would eliminate these effects and ensure good power performance.

Conclusions

In summary, a rational design involving PDA–SiO_2 composite modification of a PE separator was proposed. With a simple dip-coating process, PDA formed an overall-cover self-supporting film throughout the PE network and ceramic layer, which mechanically forms the backbone of the PE separators and amends the film-forming properties of the separator. By combining the functions of the ceramic and PDA, we showed that the developed composite-modified separator displayed substantially enhanced thermal and mechanical stability. The cells assembled with the developed separators showed excellent safety performance, which will be promising for LIB applications requiring high safety features. Furthermore, this composite modification method suggests new avenues to improve the safety performance of LIBs. Considering that ceramic-coated separators are increasingly being adopted in the large-scale application of LIBs, this rationally designed modification strategy will be very promising for industrialization.

Acknowledgements

This work was financially supported by the National Natural Science Foundation of China (Grant No. 21503180, 21273185 and 21321062) and the Fundamental Research Funds for the Central Universities (20720140513). We thank Zhiqiang Zhao in Xiamen University for pouch cells manufacture.

References

1 B. Scrosati, J. Hassoun and Y.-K. Sun, *Energy Environ. Sci.*, 2011, **4**, 3287–3295.
2 T.-H. Kim, J.-S. Park, S. K. Chang, S. Choi, J. H. Ryu and H.-K. Song, *Adv. Energy Mater.*, 2012, **2**, 860–872.
3 A. Zhamu, G. Chen, C. Liu, D. Neff, Q. Fang, Z. Yu, W. Xiong, Y. Wang, X. Wang and B. Z. Jang, *Energy Environ. Sci.*, 2012, **5**, 5701–5707.
4 J. M. Tarascon and M. Armand, *Nature*, 2001, **414**, 359–367.
5 J. Wen, Y. Yu and C. Chen, *Mater. Express*, 2012, **2**, 197–212.
6 M. M. Thackeray, C. Wolverton and E. D. Isaacs, *Energy Environ. Sci.*, 2012, **5**, 7854.
7 P. Arora and Z. Zhang, *Chem. Rev.*, 2004, **104**, 4419–4462.
8 H. Lee, M. Yanilmaz, O. Toprakci, K. Fu and X. Zhang, *Energy Environ. Sci.*, 2014, **7**, 3857–3886.
9 S. S. Zhang, *J. Power Sources*, 2007, **164**, 351–364.
10 H.-J. Ha, E.-H. Kil, Y. H. Kwon, J. Y. Kim, C. K. Lee and S.-Y. Lee, *Energy Environ. Sci.*, 2012, **5**, 6491–6499.
11 D. Y. Oh, Y. E. Choi, D. H. Kim, Y.-G. Lee, B.-S. Kim, J. Park, H. Sohn and Y. S. Jung, *J. Mater. Chem. A*, 2016, **4**, 10329–10335.
12 J. Zhang, J. Zhao, L. Yue, Q. Wang, J. Chai, Z. Liu, X. Zhou, H. Li, Y. Guo, G. Cui and L. Chen, *Adv. Energy Mater.*, 2015, **5**, 1501082.
13 E. Quartarone and P. Mustarelli, *Chem. Soc. Rev.*, 2011, **40**, 2525–2540.
14 A. Manuel Stephan, *Eur. Polym. J.*, 2006, **42**, 21–42.
15 P. G. Balakrishnan, R. Ramesh and T. Prem Kumar, *J. Power Sources*, 2006, **155**, 401–414.
16 Y. Zhu, S. Xiao, Y. Shi, Y. Yang, Y. Hou and Y. Wu, *Adv. Energy Mater.*, 2014, **4**, 1300647.
17 D. Wu, C. Shi, S. Huang, X. Qiu, H. Wang, Z. Zhan, P. Zhang, J. Zhao, D. Sun and L. Lin, *Electrochim. Acta*, 2015, **176**, 727–734.
18 M. Rao, X. Geng, Y. Liao, S. Hu and W. Li, *J. Membr. Sci.*, 2012, **399–400**, 37–42.
19 Y. S. Zhu, X. W. Gao, X. J. Wang, Y. Y. Hou, L. L. Liu and Y. P. Wu, *Electrochem. Commun.*, 2012, **22**, 29–32.
20 Y. Zhu, F. Wang, L. Liu, S. Xiao, Z. Chang and Y. Wu, *Energy Environ. Sci.*, 2013, **6**, 618–624.
21 H.-S. Jeong and S.-Y. Lee, *J. Power Sources*, 2011, **196**, 6716–6722.
22 Y. Lee, H. Lee, T. Lee, M.-H. Ryou and Y. M. Lee, *J. Power Sources*, 2015, **294**, 537–544.
23 H. Liu, Z. Dai, J. Xu, B. Guo and X. He, *J. Energy Chem.*, 2014, **23**, 582–586.
24 J.-H. Park, W. Park, J. H. Kim, D. Ryoo, H. S. Kim, Y. U. Jeong, D.-W. Kim and S.-Y. Lee, *J. Power Sources*, 2011, **196**, 7035–7038.
25 F. Croce, M. L. Focarete, J. Hassoun, I. Meschini and B. Scrosati, *Energy Environ. Sci.*, 2011, **4**, 921.
26 C. Shi, P. Zhang, L. Chen, P. Yang and J. Zhao, *J. Power Sources*, 2014, **270**, 547–553.
27 P. Yang, P. Zhang, C. Shi, L. Chen, J. Dai and J. Zhao, *J. Membr. Sci.*, 2015, **474**, 148–155.

28 P. Zhang, L. Chen, C. Shi, P. Yang and J. Zhao, *J. Power Sources*, 2015, **284**, 10–15.
29 L. Zhang, Z. Liu, G. Cui and L. Chen, *Prog. Polym. Sci.*, 2015, **43**, 136–164.
30 H. Lee, S. M. Dellatore, W. M. Miller and P. B. Messersmith, *Science*, 2007, **318**, 426–430.
31 M. H. Ryou, Y. M. Lee, J. K. Park and J. W. Choi, *Adv. Mater.*, 2011, **23**, 3066–3070.
32 M.-H. Ryou, D. J. Lee, J.-N. Lee, Y. M. Lee, J.-K. Park and J. W. Choi, *Adv. Energy Mater.*, 2012, **2**, 645–650.
33 S. M. Kang, N. S. Hwang, J. Yeom, S. Y. Park, P. B. Messersmith, I. S. Choi, R. Langer, D. G. Anderson and H. Lee, *Adv. Funct. Mater.*, 2012, **22**, 2949–2955.
34 H. Lee, B. P. Lee and P. B. Messersmith, *Nature*, 2007, **448**, 338–341.
35 M.-H. Ryou, J. Kim, I. Lee, S. Kim, Y. K. Jeong, S. Hong, J. H. Ryu, T.-S. Kim, J.-K. Park, H. Lee and J. W. Choi, *Adv. Mater.*, 2013, **25**, 1571–1576.
36 W.-H. Zhou, C.-H. Lu, X.-C. Guo, F.-R. Chen, H.-H. Yang and X.-R. Wang, *J. Mater. Chem.*, 2010, **20**, 880–883.
37 J. P. Bothma, J. de Boor, U. Divakar, P. E. Schwenn and P. Meredith, *Adv. Mater.*, 2008, **20**, 3539–3542.
38 M. d'Ischia, A. Napolitano, A. Pezzella, P. Meredith and T. Sarna, *Angew. Chem., Int. Ed.*, 2009, **48**, 3914–3921.
39 W. Stoeber and A. Fink, *J. Colloid Interface Sci.*, 1968, **26**, 62–69.
40 J. H. Waite, *Nat. Mater.*, 2008, **7**, 8–9.
41 Q. Ye, F. Zhou and W. Liu, *Chem. Soc. Rev.*, 2011, **40**, 4244–4258.
42 C. Cao, L. Tan, W. Liu, J. Ma and L. Li, *J. Power Sources*, 2014, **248**, 224–229.
43 G. C. Li, H. K. Jing, Z. Su, C. Lai, L. Chen, C. C. Yuan, H. H. Li and L. Liu, *J. Mater. Chem. A*, 2015, **3**, 11014–11020.
44 B. D. McCloskey, H. B. Park, H. Ju, B. W. Rowe, D. J. Miller and B. D. Freeman, *J. Membr. Sci.*, 2012, **413–414**, 82–90.
45 C. Daniel, *JOM*, 2008, **60**, 43–48.
46 Y. M. Shin, Y. B. Lee and H. Shin, *Colloids Surf., B*, 2011, **87**, 79–87.
47 M. Sureshkumar, P.-N. Lee and C.-K. Lee, *RSC Adv.*, 2012, **2**, 5127–5129.